Turkish Journal of Electrical Engineering & Computer Sciences

http://journals.tubitak.gov.tr/elektrik/

Research Article

Turk J Elec Eng & Comp Sci
(2022) 30: 2073 – 2085

doi:10.55730/1300-0632.3925

A conical-beam dual-band double aperture-coupled stacked elliptical patch antenna design for 5G

Feza Turgay ÇELİK[1], **Kamil KARAÇUHA**[2,*]
[1]Department of Electrical and Electronics Engineering, Faculty of Engineering, Middle East University, Ankara, Turkey
[2]Department of Electrical and Electronics Engineering, Faculty of Engineering, İstanbul Technical University, İstanbul, Turkey

Received: 31.01.2022 • **Accepted/Published Online:** 02.06.2022 • **Final Version:** 28.09.2022

Abstract: This study investigates a dual-band, aperture coupled and stacked elliptical patch antenna with conical radiation. To obtain such characteristics, the TM_{21} mode of the radiating elliptical patches is excited by utilizing two special apertures and shorting planes. The proposed antenna operates both at 2.45 GHz and 3.5 GHz. The design aims to be used indoor applications of 5G operating in both free and planned 5G bands, respectively. Therefore, the low-profile antenna element that has a monopole-like radiation pattern is a good candidate for two-dimensional arraying. The design steps and the evolution of the proposed antenna are presented in detail. The simulation and experimental results reveal many similarities regarding the scattering parameters, radiation patterns, and gain. The scattering parameter, $|S_{11}|$ is less than -10 dB in both operating bands. Novelties of the proposed study are the configuration and choice of the apertures as well as stacking structure and miniaturization techniques in elliptical patches.

Key words: Antenna design, aperture, conical beam radiation, elliptical patch, mode analysis, stacked patch

1. Introduction

With 5G technology, connectivity between human to human, human to machine, and machine to machine is expected to increase remarkably. To handle such demands, the service providers and the manufacturer should deal with the performance of the components employed in this process, extensively. Since the antenna design plays a key role, the investigation and research focus on this subject is expected. Recently, the radiation pattern reconfigurability, compactness, mass manufacturability in low profile structures, energy efficiency, eco-friendly producibility, and equal distribution to end-users are the key points for the researchers. Also, researchers have different additional parameters, including theoretical limits, hybrid approaches in high-frequency computation electromagnetics, substrate doping [1, 2]. Besides these facts, changes in human lifestyle drive the researchers to focus on dual-band antenna designs since it is common in daily life to connect both to Wi-Fi and service providers, simultaneously operating in different frequency bands. In near future, all machines for indoor applications can be controlled remotely via 5G and Wi-Fi bands [1–4]. To achieve the aforementioned technological steps by considering the energy efficiency, mass manufacturability in low profile structures, and suitability of the antenna element for arraying, the antenna design for a new generation of technology is an important topic for both academic and commercial interests. Therefore, the present study aims to design such an antenna that can be employed indoor applications. This study examined a dual-band elliptic patch antenna design and modal

*Correspondence: karacuha17@itu.edu.tr

analysis for Wi-Fi and 5G band. The antenna design is considered for smart homes operating in two frequency bands. In the low-frequency band (2.45 GHz), indoor devices would communicate with each other, while the high-frequency band (3.5 GHz) would provide communication with the operators, allowing remote control.

Current study makes calculations according to a model assuming patches as cavities [5–10]. Each mode has its characteristics of radiation pattern due to the current induced on the surfaces of the corresponding cavity [11]. In the literature, dual-band aperture coupled single-fed elliptical patch design operating at TM_{21} has not been studied extensively. In recent studies regarding the stacked antenna structures, band filtering and radiation zeroing have been employed to obtain required S-parameters keeping the radiation pattern the same in the frequency band [12–14]. In [15, 16], the elliptical patch stacked structures have been utilized. However, these structures were designed for circularly polarized performance. Our proposed work differs from the issues mentioned above by several points. First, the aperture coupling is employed on the radiating patch while minimizing the dimensions and the radiation distortion. Besides, two apertures are employed to have dual-band characteristics, and TM_{21} mode is excited on both patches.

The present study aims to design a dual-band antenna with conical-beam radiation. Since at the corresponding TM_{21} mode, the current on the metallic surfaces is concentrated outer part of the surface whereas, the current at the center is canceled, the required beam form is obtained [17–20]. Besides, to have a compact design, broader bandwidth, and also due to the limitation of the dimensions, the stacked architecture is preferred [21, 23]. For indoor applications, monopole-like radiation with a low-profile antenna can be appealing due to practical issues. There exist two patches for two different bands placed on top of each other separated from a dielectric material. By two apertures, two patches are excited by a single-fed transmission line. These apertures are designed such that the first one is suitable for a wider frequency range, including both required bands, whereas another is specifically designed for the higher frequency regime (3.5 GHz). There are several factors that yield asymmetry in conical beam patterns such as having two metallic surfaces on top of each other and asymmetric aperture positioning. To avoid such a phenomenon, the asymmetric localization of the slots and stubs are inserted. Getting rid of this problem also leads to the miniaturization of the geometries. Parametric analysis for each step (cavity modes, miniaturization, aperture design) is performed to understand the effect of antenna dimensions and structure on its performance. Then, the prototype is produced, and measurements of scattering parameters, radiation patterns, and gain values are provided. Experiments validate the simulation.

The structure of the present study is as follows. In Section 2, the theoretical background of the antenna structure is given. The section explains the cavity model, apertures, and design constraints in detail. Then, the simulations and their results are given in Section 3 where the discussion on the approaches is provided with the parametric investigation. After that, the conclusion would be drawn in Section 4.

2. Antenna design

In this section, theoretical backgrounds of the patches, a preliminary study about the ellipse excitation and finally, the details of the proposed antenna are provided.

2.1. Theoretical background

In this study, elliptical geometry is selected as antenna shape; and elliptical microstrip patch type antennas are put under investigation. As a microstrip structure is selected, a cavity model can be used to understand the radiation phenomenon of the antenna. The cavity model is a model that converts a microstrip antenna problem into a closed cavity one. We use perfect electric conducting (PEC) walls as top and bottom conductors

of the antenna and perfect magnetic conducting (PMC) walls for the dielectric sides in this type of model [23]. When the antenna is placed on the x-y plane, the cavity model yields a series of TM modes. The sequence of TM modes for the elliptical patch as TM_{11}, TM_{21}, TM_{02}, etc. [23]. To have a better understanding, surface current distributions of the first two modes for an arbitrary elliptical patch are provided in Figure 1. The cavity model of the patch antennas enables us to use approximate relations to design a printed antenna. In this paper, the resonance frequency relations for elliptic patch structures are used. The size and axial ratio of the elliptical patch are determined by using approximate formulas given in (1) and (2):

$$f_r = \frac{c\sqrt{q}}{\pi a e\sqrt{\varepsilon_r}} \tag{1}$$

$$e = \sqrt{1 - \left(\frac{b}{a}\right)^2} \tag{2}$$

Here, c is the speed of the light, ε_r is the relative permittivity of the dielectric substrate, a and b are the half-length of the major and minor axis of the corresponding elliptical structure, respectively [23]. The variable q stands for the argument of the modified Mathieu function as given in [23].

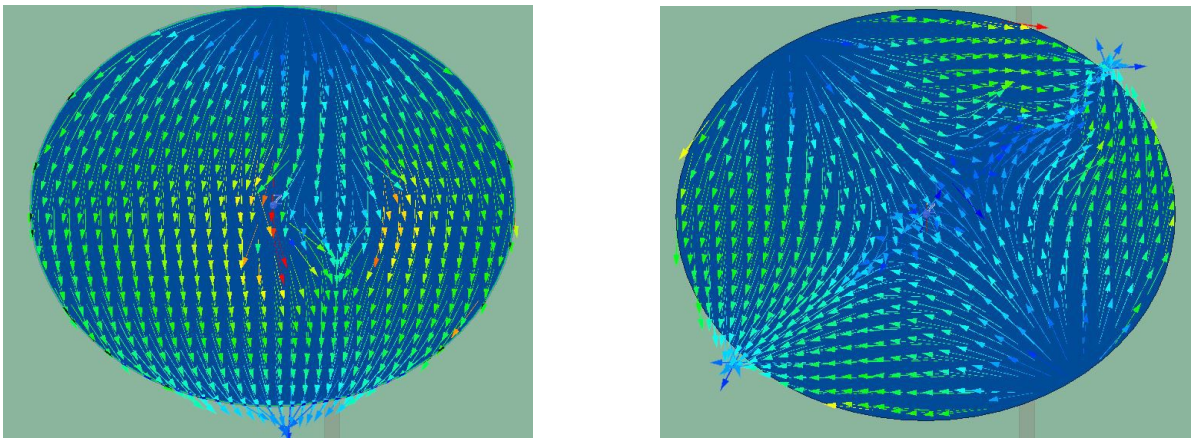

(a) (b)

Figure 1. The surface current distributions of the first two modes of an elliptical patch ((a) TM_{11}, (b) TM_{21}).

To obtain conical beam radiation, the TM_{21} mode of the antenna is excited. Therefore, q_{21} needs to be found. The resonance frequency of the antenna is calculated by applying PMC boundary condition to the Electric field at the boundaries of the antenna. Electrical field expressions at the elliptic patch antenna use the modified Mathieu function. Therefore, to satisfy the Neumann boundary condition on the antenna edge, a derivative of the modified Mathieu function must be equated to zero. As the evaluation steps of this function are challenging and we only need the argument of function (q) which makes the derivative of this function zero, approximate formulas for q will be used instead of evaluating function. The polynomial approximation of q_{12} can be found as (3):

$$q_{21} = -0.006e + 2.149e^2 + 0.9476e^3 - 0.0532e^4 \tag{3}$$

In this expression q_{21} is applicable for TM_{21} mode of operation. The expression given in (3) is a valid approximation if e value provided in (2) is between 0.42 and 1.0 [23]. Therefore, the expressions illustrated

above are studied iteratively. The iterations aim to satisfy (1) at 2.45 and 3.5 GHz values. Iterations start with initial a and b values. Then, according these values e, q and f_r are calculated. Depending on the f_r value, a and b are updated. After several iterations, approximate values of a and b lengths are found. Then, the elliptic patch is simulated by employing ANSYS HFSS software. The calculated a and b values do not yield resonance at exactly target frequencies (2.45 and 3.5 GHz). Therefore, a parametric study on these lengths is studied.

This study is mainly focused on conical beams. In order to obtain a conical beam, the TM_{21} mode of the antenna should be preferred. As TM_{21} is a second mode, its resonance frequency is quite large compared to the first mode. The increase in the resonance frequency yields an increase in the electrical size of the antenna. Therefore, several antenna miniaturization techniques should also be studied to keep the antenna reasonably sized.

2.2. Preliminary study

In search of a conical beam, an additional mode that the cavity model does not predict is excited [24]. This mode divides the antenna into two portions by creating a current null at its center. This mode's surface current and E-field distribution resemble the TM_{02} mode of the rectangular patch [11]. As this additional mode has the same symmetric E-field at both radiating edges, the radiated field has a conical shape. The surface current distribution and radiation pattern of the antenna can be seen in Figure 2. This mode can be excited with a unique feeding mechanism. The proximity coupled feeding type located right in the middle section of the ellipse achieves such excitation. The feed position can be seen in Figure 2.

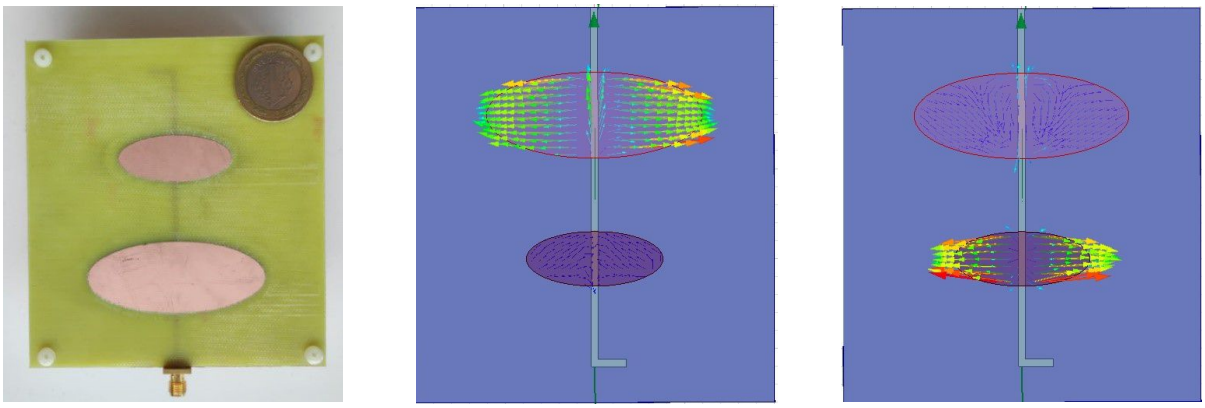

(a) (b) (c)

Figure 2. The top view (a) and the corresponding current distributions (b) 2.45 GHz, (c) 3.6 GHz.

The designed antenna is fabricated, simulated, and measured. The radiation patterns of the antenna can be found in Figure 3.

The corresponding figure compares the measurement results with the simulated ones. As investigated in [24], the preliminary work on the elliptical radiators is analyzed. According to this analysis, we have encountered that the conical beam can be obtained by enforcing current nullification. To achieve this aim, a proximity-coupled feeding structure passing the middle section of the elliptical patch is preferred. Since such a forcing feeding approach is utilized, the surface current and resulting radiation patterns are obtained as seen in Figure 2 and Figure 3. As can be understood from the measurement results, the antenna illustrates a

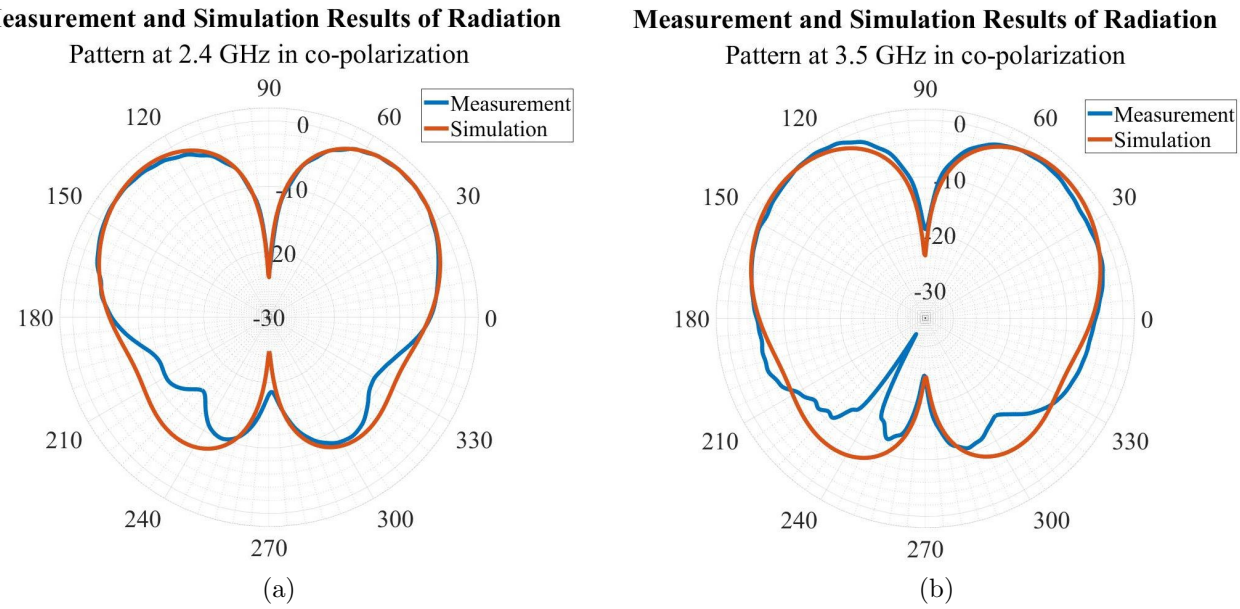

Figure 3. Radiation patterns for $\phi = 0^0$ plane.

remarkable resemblance with the simulation outcomes. Although the antenna is matched at 2.45 and 3.5 GHz points, it supports these resonances at a very narrow frequency band. As the excitation is made forcefully, it can excite the antenna only in a narrow band. Therefore, the following antenna is proposed such that it should have a similar radiation pattern with a wider frequency bandwidth, especially in the higher frequency band.

2.3. Proposed antenna

After conical beam operation with the symmetric mode, as illustrated in the previous section, it is understood that the antenna should be excited with the corresponding TM mode to have a more stable resonance and broader bandwidth. This observation yields TM_{21} mode as a possible candidate for the conical beam. As it is seen in Figure 4, the currents are canceled in the middle of the radiating elements, and currents are maximized at the edges. The elliptical patch can be miniaturized to have a smaller size by preserving TM_{21} properties. This study prefers the current mode enlargement technique as a miniaturization technique. In order to make the current path larger, one should decide the positions of the current nulls on the patch. As TM_{21} has four symmetric current nulls, they are placed at the corners of the antenna by thinking the antenna has a rectangular shape. After deciding on current null points, the current lines are drawn between these points. The positions of slots are arranged to coincide with the middle section of the surface currents. In this way, the currents are forced to take a larger path. In addition to the slots, to make further miniaturization, the positions of the current null points are changed. These positions of the current nulls are changed by adding small stubs at the null points. The corresponding three-dimensional far-field radiation patterns are provided for two different resonances in Figure 5. The resultant antenna achieved miniaturization. The top and isometric views of the miniaturized antenna can be found in Figure 6. The corresponding dimensions are tabulated in Table 1.

Although the large antenna size is prevented by antenna miniaturization, we still have to address the narrow bandwidth (BW) of the antenna. As the antenna operates in TM_{21} mode, narrow BW is expected and can be enhanced with different excitation methods. In this study, an aperture coupling mechanism is preferred. Here, the aperture shape that enables wider bandwidth is investigated. Several aperture types and sizes are

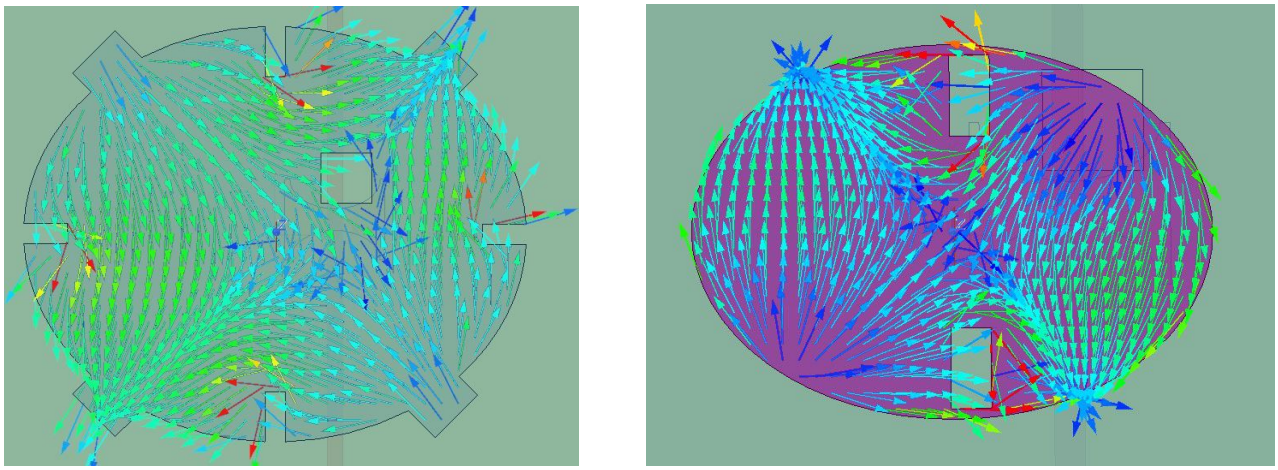

(a) (b)

Figure 4. Surface currents of the larger (a) (Layer-4) and smaller (b) (Layer-5) patches.

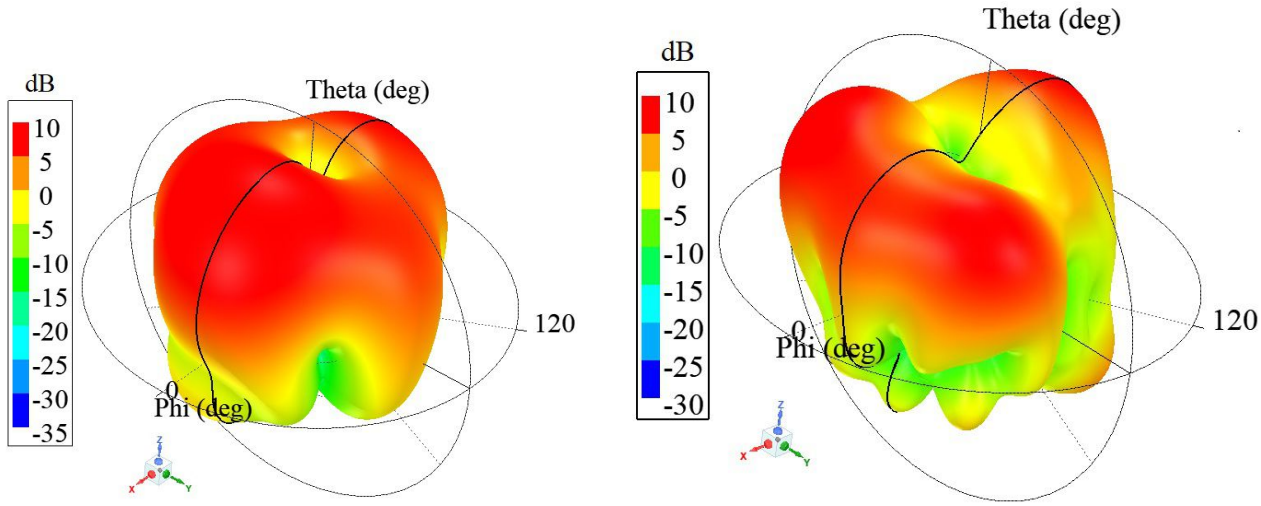

(a) (b)

Figure 5. 3-dimensional raditation pattern for (a) 2.4 GHz and (b) 3.5 GHz.

studied, such as narrow rectangular slots, wide rectangular slots, H-shaped slots, and continuously tapered slots [25]. The continuously tapered slot provides the widest bandwidth among all other types. In this slot, the aperture starts narrow and widens by following the equation of an ellipse. The continuously tapered aperture can be seen from the fabricated prototype in Figure 7. When the aperture selection and antenna miniaturization are done, the resonance at 2.45 GHz having conical beam is achieved successfully. After obtaining the desired radiation, the study now focuses on performance at 3.5 GHz. As the frequency difference between bands (2.45 and 3.5 GHz) is large, another radiator is required for the second band. An additional radiator is placed as a second layer to the elliptic patch to save space. In order to supply broadened bandwidth to the smaller patch, another aperture coupled feed structure is constructed. Here, the aperture is carved on a large ellipse structure. At this point, the position of the second aperture plays a crucial role. The radiation phenomenon of the larger patch is explained by surface currents that flow closer to the antenna's edge. In order not to disturb these currents, the second aperture is placed away from the edges. The apertures can be found in Figure 7.

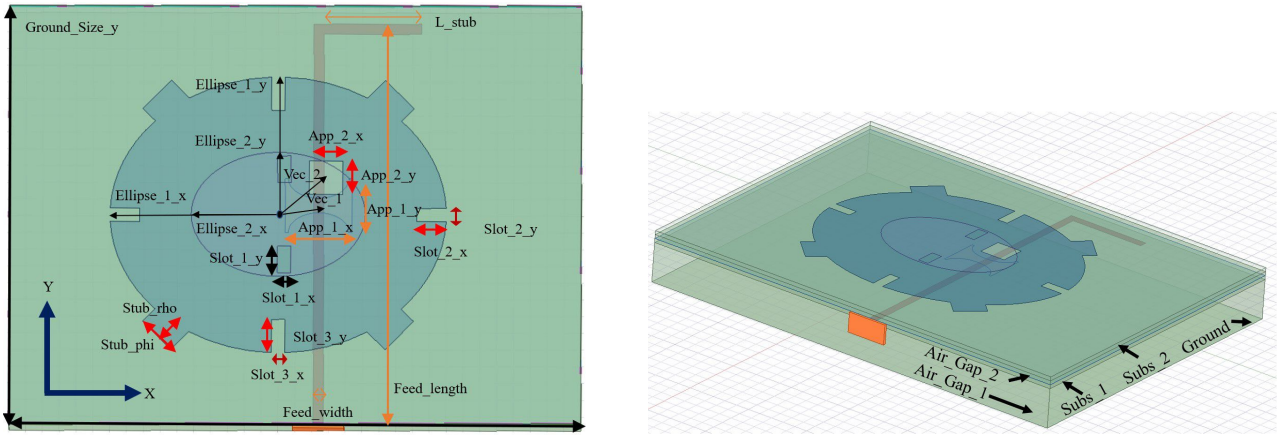

(a) (b)

Figure 6. Top (a) and isometic view (b) of the stacked antenna group.

Table 1. Antenna parameters and their dimensions.

Parameters	Dimension in mm	Parameters	Dimension in mm
Ground_Size_y	125	Stub_phi	8.50
Ground_Size_x	170	Stub_rho	5.8
Ellipse_1_x	50	Slot_1_x	4
Ellipse_1_y	41.40	Slot_1_y	8
Ellipse_2_x	25.90	Slot_2_x	8.7
Ellipse_2_y	18.50	Slot_2_y	4
L_stub	32	Slot_3_x	4
Feed_length	120	Slot_3_y	10
Feed_width	3.05	Vec_1	(12.20, 3.20)
App_1_x	19.95	Vec_2	(14.20, 11.20)
App_1_y	16	Subs_1_z_size	1.524
App_2_x	10	Subs_2_z_size	1.524
App_2_y	10	Air Gaps	15 & 1.5

The second antenna designed to operate at 3.5 GHz is also fed by using the aperture coupling phenomenon. This study aims to create an antenna that radiates conical beam at both its resonance points; the second elliptical patch antenna is also needed to operate at TM_{21} mode. To have a symmetric pattern with respect to the first ellipse, the null points of the surface currents are selected at the same position as the first antenna. To guarantee all positions of the null points at the theoretically predefined locations, both antennas are soldered to the aperture plate (which behaves like the ground of all structures) by a conducting strip. This conducting strip is placed to connect center points of the upper ellipse, lower ellipse, and aperture plate. An optometric analysis of the HFSS arranges the position of the shorting strip. At this optimization, the size of the strip and its position are considered design parameters where the symmetry of the far-field of the pattern is used as a performance parameter of the optimization. The analysis is arranged to get the most symmetric conical beam possible.

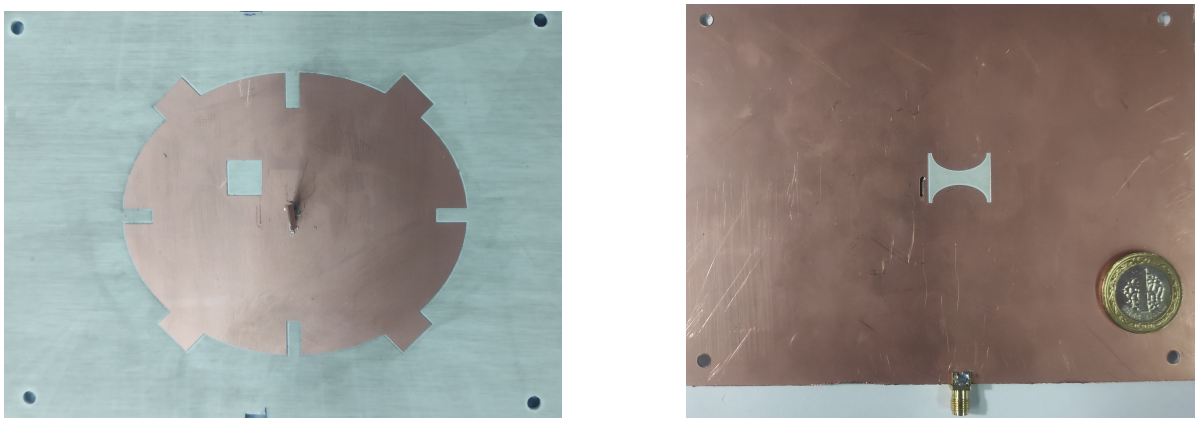

(a) (b)

Figure 7. Top view of the fabricated patch and aperture. Layer-4 (a) and Layer-3 (b).

Notice that the second antenna is placed on top of the first ellipse. This configuration is applicable as the conical beam already introduced a null point in broadside direction. However, placing a metallic element comparable to the original antenna diverts the radiation pattern and distorts the pattern shape. In order to minimize pattern distortion, the second elliptical patch must be miniaturized. The second antenna is miniaturized by adding slots on top of it. These slots extend the path traveled by the surface currents, thus reducing the antenna size. The top layer is provided in Figure 8.

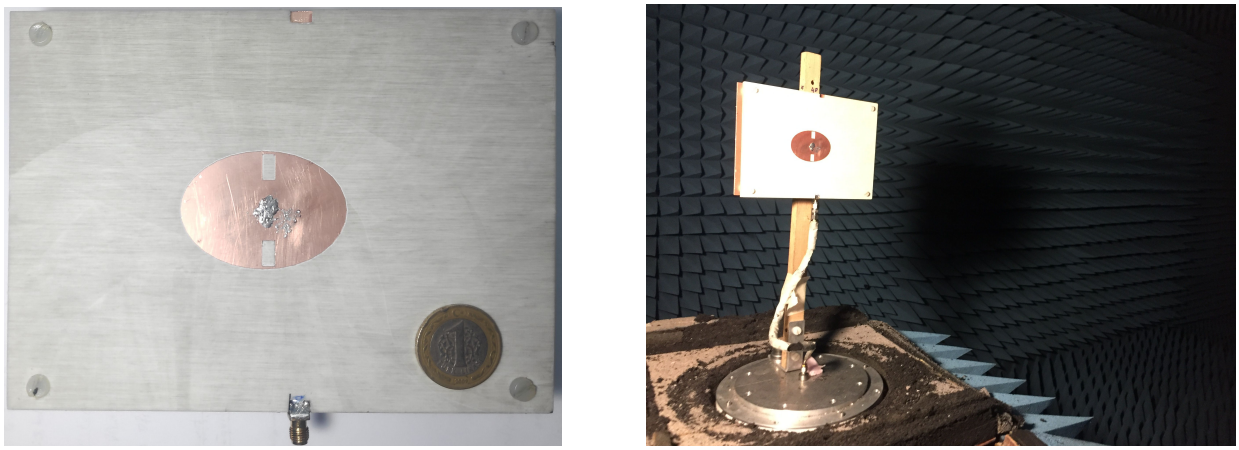

(a) (b)

Figure 8. Top view of the fabricated patch (Layer-5) (a) the radiation pattern measurement setup (b).

3. Numerical and experimental results

The prototype of the designed antenna is fabricated by using an LPKF H100 Promat milling machine. The substrate of the patches is selected as Rogers 4003 ($\varepsilon_r = 3.55$ and $\tan\delta = 0.009$), which has a thickness of 1524 mm. The structure consists of two dielectric plates, two air gaps, and a reflector plate. As the antenna is composed of five layers, it may be challenging to understand it. Let us investigate layers one by one. The bottom layer is a rectangular copper plate, which prevents back radiation due to the excitation line. After this

layer, an air gap of 15 mm is placed. Then, the second layer, which contains the signal line, is introduced. The width of this signal line is arranged to yield 50 Ω when it is used as a microstrip line having dielectric properties illustrated above. After the signal line, the aperture that couples electromagnetic energy to the elliptical patches is located as the third layer. The aperture size and shape are optimized to get the broadest band possible for both resonators. The aperture is separated from patches by an air gap. This gap is selected as air to increase the bandwidth of the antenna by reducing the effective dielectric constant of the structure. After the air gap antenna employs its fourth layer that includes a printed dipole of the elliptical patch, this patch is arranged to resonate its TM_{21} mode in 2.45 GHz. In addition to its miniaturization elements, this antenna is milled by a rectangular slot to enable aperture coupling to the second antenna. The fifth and final layer of the antenna employs an elliptical patch that operates at 3.5 GHz. The corresponding antenna is excited by an electromagnetic field that passes through two consecutive apertures. The layout of the antenna system and the shapes of the layers can be seen in Figure 7 and Figure 8. The prototype antenna is tested to obtain its performance parameters. In this content $|S_{11}|$, radiation patterns in $\phi = 0^0$ cut and maximum gain measurements are taken. Measurement and simulated $|S_{11}|$ values of the antenna can be seen in Figure 9.

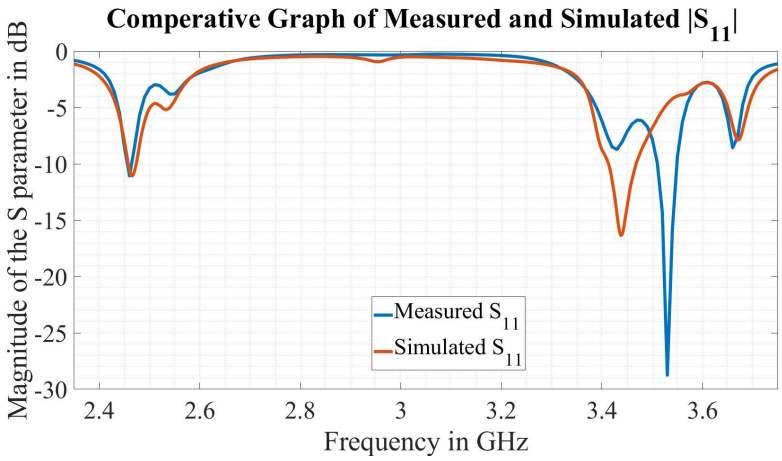

Figure 9. Measured and simulated $|S_{11}|$ parameters.

The $|S_{11}|$ measurements illustrate the dual-band operation of the antenna at 2.45 and 3.5 GHz points. The measurement results of the antenna at 2.45 GHz perfectly match the simulation results. There is some frequency shift at the larger frequency. This frequency shift occurs as a result of the fabrication process. The smaller patch structure has very narrow conductor lines. These narrow lines are created by the slots that miniaturize the antenna. As the conducting parts are narrow, there exist fabrication mistakes. As these mistakes were foreseen earlier, the operation frequency of the antenna is shifted in the simulation environment. That is why the antenna operates at 3.45 GHz in simulations instead of 3.5 GHz. The fabricated antenna resonates at the correct frequency band as we anticipated possible frequency shifts earlier. The S parameter graph shows us the bandwidths of both frequencies. In this antenna, there is a limitation on the bandwidths due to the different sizes of the patches. The lower frequency patch can excite the broadband when the aperture is placed far from its center. However, this kind of feeding makes it impossible to etch another aperture and feed the other patch. So the band of the 2.45 GHz is kept narrow utilizing the exciting upper patch in a broader band. This choice is applicable in our application as the narrowband would be sufficient to operate in the Wi-Fi region. The radiation patterns of the antenna are measured at $\phi = 0^0$ plane. The study aims to obtain a conical beam for

both frequencies. The measured and simulated radiation patterns of the antenna can be seen in Figure 10.

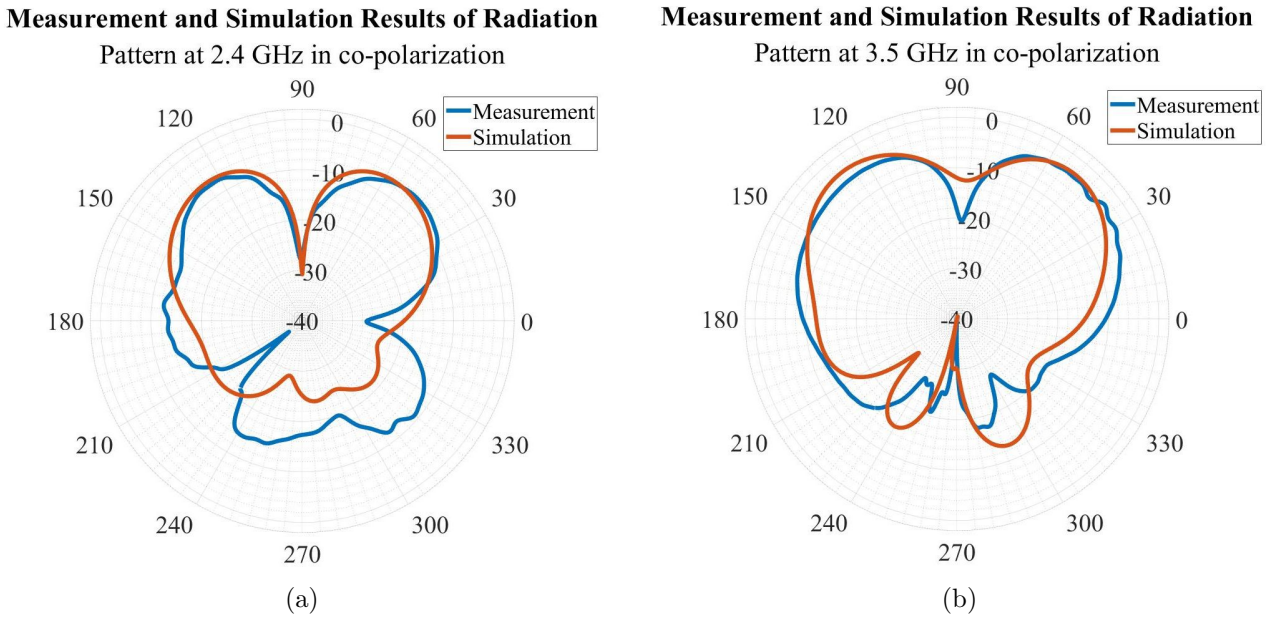

Figure 10. Radiation patterns for $\phi = 0^0$ plane.

The elliptical patches are designed to be used in linear polarization. The excitation is done to support linear polarization. The polarization phenomenon of the antenna can be studied by investigating its co and cross-polarization pattern measurements. The co and cross-polarization patterns of the antenna are given in Figure 11.

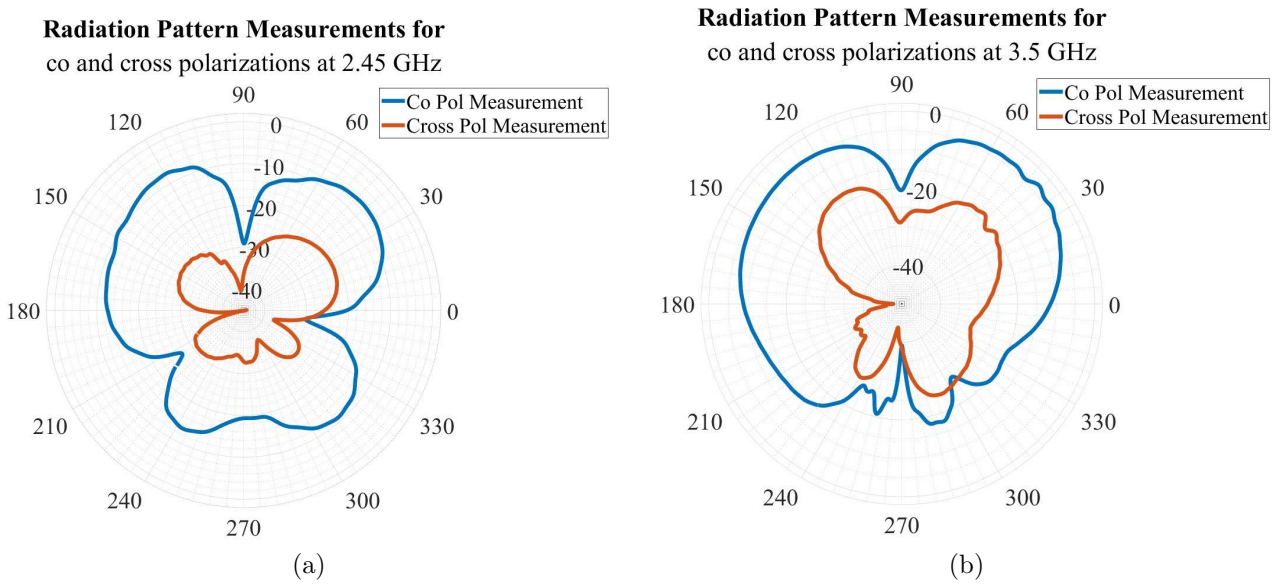

Figure 11. Co- and cross-radiation patterns for $\phi = 0^0$ plane.

As shown in Figure 11, the difference between co and cross-polarized powers is larger than the 10 dB.

This proves that the designed antenna operates in linear polarization. After measuring the radiation pattern of the antenna, the maximum gain values of it are measured. The three antenna method is used to take the gain measurement. According to this method, the antenna's gain under test is calculated by taking measurements with a standard gain antenna. The measured gain values for both frequencies can be found in Table 2.

Table 2. Maximum realized gain measurements.

Realized gain (dBi)	Frequency = 2.45 GHz	Frequency = 3.5 GHz
Simulation	7.05	5.77
Experiment	6.50	5.22

As it can be seen from the measured gain values, 2.45 GHz has a more significant value. The difference between gain values can be understood by inspecting the radiation patterns of the antennas. The initial expectation was to observe higher gain at a high-frequency application. This expectation is applicable if the radiation patterns of both frequencies have the same shape. However, the radiation pattern of our antenna illustrates several differences at 2.45 and 3.5 GHz. When the radiation pattern of 3.5 GHz is investigated, broader beams and higher broadside radiation values can be seen. These differences divert focusing of input power, thus reducing the maximum gain value.

4. Conclusion

The primary motivation of the study is to investigate elliptical patches with double aperture type excitement and the miniaturization for dual-band operations having conical radiation. As far as we know, such an approach has not been studied yet. Therefore, the present study would fill this literature gap and constitute an essential start for new studies on these issues. In this study, a conical-beam dual-band double aperture-coupled stacked elliptical patch antenna design was studied. The present study proposes a low-profile dual-band stacked patch antenna design with monopole-like radiation, including a novel excitation approach. The design could be employed indoor application of smart houses and 5G technology due to its corresponding dual-band nature. The lower frequency band is suitable for the Wi-Fi band, whereas the higher frequency regime would be available for 5G. The shapes in the antenna regarding the radiating patches, apertures, slots, and stubs are chosen considering both manufacturability and novelty. There exist advantages and disadvantages to the stacked structures. Bandwidth broadening and compactness are the advantages of the approach and are employed in the design. The disadvantages, such as the interaction of the elements and the deterioration of the radiation pattern, are eliminated by choosing proper apertures, localization of the patch, slots, and stubs. Two antenna miniaturization techniques are utilized since the design is initially planned to be employed in a linear array structure. These miniaturization techniques are slot and stub employment, taking into account the minimum and maximum induced current at the required mode for both patches. The design steps and the evolution of the proposed antenna are presented in detail. The simulation and experimental results reveal many similarities regarding the scattering parameters, radiation patterns, and gain. The scattering parameter, $|S_{11}|$ is less than -10 dB in the operating bands. The radiation pattern and maximum realized gains are in harmony with the simulation and experiment.

Acknowledgment

The authors of the paper would like to express gratitude to Damla Alptekin Soydan, Assoc. Prof Dr. Fatih Dikmen, Prof. Dr. Özlem Aydın Çivi, and Prof. Dr. Ertuğrul Karaçuha for their useful discussions. This work is supported in part by İstanbul Technical University (ITU) Vodafone Future Lab under project no. ITUVF20180901P10. It should be highlighted that the measurements were conducted at the Electrical and Electronics Engineering Department of Middle East Technical University.

References

[1] Çelik FT, Karaçuha K. Miniaturized virtual array dual band loop quasi-yagi antenna design for 5G application. In: URSI International Symposium on Electromagnetic Theory; San Diego, CA, USA; 2019. pp. 1-4.

[2] Çelik FT, Karaçuha K. A Reconfigurable binomial weighted phased array antenna design for Wi-Fi band. In: 2020 Signal Processing and Communications Applications Conference; Gaziantep, Turkey; 2020. pp. 1-4.

[3] Çelik FT. Pattern reconfigurable antenna designs in sub-6 ghz band for 5G applications. MSc, Middle East Technical University, Ankara, Turkey, 2021.

[4] Pal A, Mehta A, Mirshekar-Syahkal D, Nakano H. A twelve-beam steering low-profile patch antenna with shorting vias for vehicular applications. IEEE Transactions on Antennas and Propagation 2017; 65 (8): 3905-3912.

[5] Erbaş CD. Parametric analysis of angular rotation for microstrip patch antenna with elliptical patch and parasitic elements. In: IEEE International Conference on Electrical, Communication, and Computer Engineering; Istanbul, Turkey; 2020. pp. 1-6.

[6] Sun L, Zhang GX, Sun BH, Tang WD, Yuan JP. A single patch antenna with broadside and conical radiation patterns for 3G/4G pattern diversity. IEEE Antennas and Wireless Propagation Letters 2015; 30: 15433-15436.

[7] Liu S, Wu W, Fang DG. Wideband monopole-like radiation pattern circular patch antenna with high gain and low cross-polarization. IEEE Transactions on Antennas and Propagation 2016; 64 (5): 2042-2045.

[8] Chen SH, Row JS, Wong KL. Reconfigurable square-ring patch antenna with pattern diversity. IEEE Transactions on Antennas and Propagation 2007; 55 (2): 472-475.

[9] Liu J, Xue Q, Wong H, Lai HW, Long Y. Design and analysis of a low-profile and broadband microstrip monopolar patch antenna. IEEE Transactions on Antennas and Propagation 2012; 61 (1): 11-18.

[10] Dumanlı S. Pattern diversity antenna for on-body and off-body WBAN links. Turkish Journal of Electrical Engineering and Computer Science 2018; 26 (5): 2395-2405.

[11] Balanis CA. Antenna Theory: Analysis and Design. Hoboken, NJ, USA: John Wiley & Sons, 2015.

[12] Yang SJ, Pan YM, Shi LY, Zhang XY. Millimeter-wave dual-polarized filtering antenna for 5G application. IEEE Transactions on Antennas and Propagation 2020; 68 (7): 5114-5121.

[13] Wang Z, She R, Han J, Fang S, Liu Y. Dual-band dual-sense circularly polarized stacked patch antenna with a small frequency ratio for UHF RFID reader applications. IEEE Access 2020; 5: 15260-15270.

[14] Liang GZ, Chen FC, Yuan H, Xiang KR, Chu QX. A high selectivity and high efficiency filtering Antenna with controllable radiation nulls based on stacked patches. IEEE Transactions on Antennas and Propagation 2022; 70 (1): 708-713.

[15] Pathak P, Singhal PK, Rawat S. Design and analysis of modified elliptical patch in stacked arrangement for circularly polarized broadband performance. In: 2018 IEEE International WIE Conference on Electrical and Computer Engineering; Chonburi, Thailand; 2018. pp. 17-20.

[16] Konjunthes S, Chalermwisutkul S, Akkaraekthalin P, Thaiwirot W. Design and experiment of a wideband circularly polarized stacked patch antenna for universal UHF RFID readers. In: 2021 Research, Invention, and Innovation Congress: Innovation Electricals and Electronics; Bangkok, Thailand; 2021. pp. 135-138.

[17] Alhargan FA, Judah SR. A general mode theory for the elliptic disk microstrip antenna. IEEE Transactions on Antennas and Propagation 1995; 43 (6): 560-568.

[18] Lau KL, Luk KM. A wideband circularly polarized conical-beam patch antenna. IEEE Transactions on Antennas and Propagation 2006; 54 (5): 1591-1594.

[19] Foroozesh A, Shafai L. Investigation into the application of artificial magnetic conductors to bandwidth broadening, gain enhancement and beam shaping of low profile and conventional monopole antennas. IEEE Transactions on Antennas and Propagation 2010; 59 (1): 4-20.

[20] Row JS, Lin TY. Frequency-reconfigurable coplanar patch antenna with conical radiation. IEEE Antennas and Wireless Propagation Letters 2010; 9: 1088-1091.

[21] Wang Z, She R, Han J, Fang S, Liu Y. Dual-band dual-sense circularly polarized stacked patch antenna with a small frequency ratio for UHF RFID reader applications. IEEE Access 2017; 5: 15260-15270.

[22] Raheja DK, Kanaujia BK, Kumar S. A dual polarized triple band stacked elliptical microstrip patch antenna for WLAN applications. Wireless Personal Communications 2018; 100 (4): 1585-1599.

[23] Garg R, Bhartia P, Bahl IJ, Ittipiboon A. Microstrip Antenna Design Handbook. Massachusetts, USA: Artech House, 2002.

[24] Celik FT, Karaçuha K. İki bantlı ikili eliptik yama anten tasarımı ve modal analizleri. In: URSI TÜRKİYE 2021 X. Bilimsel Kongresi, 7-9 Eylül 2021, Gebze Teknik Üniversitesi; Gebze, Kocaeli, Turkey; 2021 (in Turkish).

[25] Gao SC, Li LW, Leong MS, Yeo TS. Wide-band microstrip antenna with an H-shaped coupling aperture. IEEE Transactions on Vehicular Technology 2002; 51 (1): 17-27.